A Enhanced Method to Improve Signal Reception Performance for 5G NR Physical Uplink Control Channel with Frequency Hopping Configuration

Dang-Minh Phan[1], Phuoc Nguyen T. H.[2]

[1]Wireless Broadband Equipment R&D Center
Viettel High Technology Industries Corporation, Viettel Group
[2]University of Information Technology
Vietnam National University Ho Chi Minh City

[1]Minhpd7@viettel.com.vn
[2]Phuocnth@uit.edu.vn

***Abstract*—This paper proposes a method to improve decoding performance for the Physical Uplink Control Channel (PUCCH) format 0 with intra-slot frequency hopping configuration. The proposed algorithm sums absolute values of correlation between symbols instead of summing their correlation. By this way, the phase opposition in symbols correlation can be theoretically eliminated in order to improve decoding accuracy. By applying simple but effective modification in algorithm, the proposed approach exhibits extraordinary performance to ensure all PUCCH performance requirements described in the TS 38.104 from 3GPP. Feasibility of the proposed method is verified by conducting experiment in laboratory environment with different intra-slot frequency hopping configurations and receiving antenna numbers.**

Keywords—gNodeB, 5G NR, eMMB, PUCCH decoder, frequency hopping, OFDM, MIMO

I. INTRODUCTION

Nowadays, the fifth generation of mobile communication has opened more opportunities for the wireless applications and services. For enhanced mobile broadband (eMBB) scenario, the 3GPP organization has developed a new radio-access technology 5G New Radio (5G NR), which reuses many key technologies from previous generation LTE. Moreover, enabling technologies such as mmWave spectrum bands exploitation and massive MIMO promise a revolution of 5G NR user experience [1].

In 5G NR system, physical uplink control channel (PUCCH) plays a crucial role as it supports following control functions: HARQ acknowledgment for downlink shared channel, scheduling request (SR) for uplink shared channel and channel-state information (CSI) for MIMO and beam-forming schemes. There are five formats of PUCCH for user equipment (UE) to choose depending on the payload size. For large payload, formats 2, 3, 4 are preferred since they exploit the effectiveness of Reed Muller and Polar decoders, as well as the utilization of additional reference signal for better channel estimation [2]-[4]. For smaller payload, format 0 requires less resource and can support large volume of users in one transmission time interval. However, decoding algorithm for this format has not been carefully considered.

For decoding PUCCH format 0, the study [5] proposed power-based algorithm in order to reduce the receiver complexity. The study [6] used the correlation value to detect signal. However, the case of multiple receiving antennas and frequency hopping were not considered. Similarly, [7] used the same approach as in [6] and showed that the correlation-based algorithm works more effectively than the power-based algorithm. The algorithm in [7], however, does not take into account the influence of frequency hopping between two OFDM symbols. The frequency hopping, on the one hand, mitigates the negative effect of fading channel, but on the other hand it causes the difference in initial phase between two OFDM symbols leading to the performance degradation for the algorithm in [7]. Moreover, the threshold in [7] must be premeasured, that makes the receiver not flexible in the case when levels of signal and noise power are fast changing.

In this study, we suggest a new approach to deal the problem caused by frequency hopping when two OFDM symbols are used in PUCCH format 0. Specifically, the squared correlation value of each OFDM symbol for each antenna is summed, then antenna combination is conducted.

This study aims to improve the reception performance of PUCCH format 0 with frequency hopping configuration. Two main features of the proposed detection algorithm are combination of squared correlation values of two OFDM symbols and setting a flexible deciding threshold for false alarm detection.

For this purpose, first we consider encoding and decoding structures of PUCCH format 0 with the proposed algorithm. Then, in order to confirm the reception performance of the proposed algorithm in radio-frequency channel, we suggest a practical testing system, which consists of Rohde & Schwarz SMW200A vector signal generator, Viettel remote radio unit (RRU) and baseband unit (BBU), where the proposed algorithm is implemented in the C language.

II. PUCCH FORMAT 0 IN 5G NR SYSTEM

A. Signal Generation

In 5G NR system, short PUCCH format 0 with or 2 OFDM symbols is used to provide the uplink transmission of up to two HARQ bits and one SR bit. Depending on the values of these bits and other pre-defined system parameters, one of phase-rotated sequences is selected for transmission. These phase-rotated sequences $S_{m_{CS}}[k]$ are orthogonal and generated from a common base sequence $u[k]$ with different phase rotations in frequency domain. The pre-defined system parameters, such as Hopping ID, Cell ID, and slot number,

TABLE I
RELATIONSHIP BETWEEN ROTATED PHASE AND HARQ SR BITS

HARQ bits	00	00	01	01	11	11	10	10
SR bit	0	1	0	1	0	1	0	1
m_{cs}	0	1	3	4	6	7	9	10
Rotated phase α	0	$\frac{\pi}{12}$	$\frac{\pi}{4}$	$\frac{\pi}{3}$	$\frac{\pi}{2}$	$\frac{7\pi}{12}$	$\frac{3\pi}{4}$	$\frac{5\pi}{6}$

etc., are transferred between user equipment and base station by other channels, so we will not take into account these parameters for simplicity of algorithm description.

The phase-rotated sequence $S_{m_{CS}}[k]$ for each OFDM symbol are computed as follows:

$$S_{m_{CS}}[k] = u[k]e^{jk\alpha}, 0 \le k \le 11 \quad (1)$$

where $u[k]$ is a length-12 low-PAPR base sequence, which values depend on the mentioned pre-defined system parameters, and completely described in [8]. The rotated phase α, which is indicated by cyclic shift m_{CS}, is showed in TABLE I. The more two sequences are different in rotated phase α, the larger Euclidean distance these sequences have.

The generated phase-rotated sequence, whose length of 12 corresponds to one resource block, are mapped to the resource grid. When two OFDM symbols are used for PUCCH transmission with frequency hopping, they are usually allocated to the edges of the frequency resource grid. After resource mapping with other uplink channels, the resource grid is used as the input of traditional OFDM scheme to generate radio frequency waveform for transmitting over the air from UE to BS.

Fig. 1 illustrates the resource grid, which contains two OFDM symbols carrying two phase-rotated sequences with frequency hopping configuration. For a slot with the duration of $0.5ms$, the resource grid has sizes of 3276 subcarriers in the frequency axis and 14 OFDM symbols in time domain axis. As seen in the figure, the 5^{th} OFDM symbol is located at subcarriers from 0^{th} to 11^{th}, and the following 6^{th} OFDM symbol with frequency hopping is located at subcarriers from 120^{th} to 131^{th}.

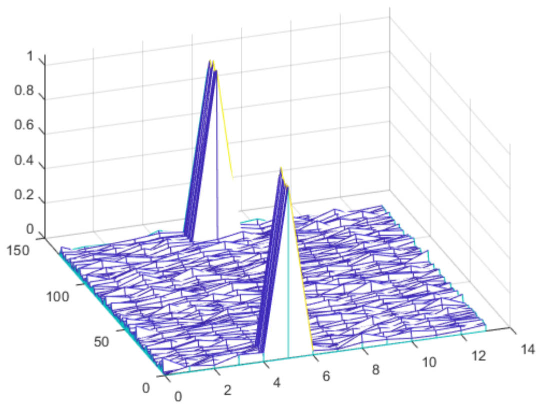

Fig. 1 Resource grid in frequency domain for PUCCH Format 0 with frequency hopping.

B. Signal Reception

At the BS side, multiple Rx antennas may be used to gain from reception diversity. The signal for each Rx antenna is independently processed, and used as the inputs for detection block. Timing synchronization between UE and BS is guaranteed by Random-Access signal [10].

In order to transmit the control information from UE to BS, the PUCCH decoder is adopted for conducting two following functions. The first task is choosing which phase-rotated sequence was sent by UE among possible sequences, then reporting the decoded HARQ and SR bits to higher layers. This task is challenging since the radio signal is affected by fading and additive white Gauss noise. The second task is to decide whether the received signal was sent by UE or there was unwanted noise (DTX detection). This can be done by using a deciding threshold, which value is chosen depending on the desired missed detection and false alarm probabilities.

For the first task, the study in [6] suggests using the highest value of squared correlation value to detect the transmitted sequence. The study [7] uses similar approach for multiple Rx antennas. According to these studies, the correlation value for each cyclic shift m_{CS} can be calculated as follows for the case of two OFDM symbols:

$$P_{m_{CS}} = \frac{1}{N_{rx}N_{Sym}N_{cs}^{RB}} \sum_{r}^{N_{rx}} \left| \sum_{i}^{N_{Sym}} \sum_{k}^{N_{cs}^{RB}} R_r^i[k]\left(S_{m_{CS}}^i[k]\right)^* \right|^2 \quad (2)$$

where: N_{rx} is the number of receiving antennas; N_{Sym} is the number of used OFDM symbols; N_{CS}^{RB} is the number of subcarriers in one resource block; $R_r^i[k]$ is the length-12 received sequence for $i-th$ OFDM symbol and $r-th$ Rx antenna; $(S_{m_{CS}}^i[k])^*$ is the complex conjugated reference sequence for $i-th$ OFDM symbol with rotated phase α defined by m_{CS} value.

When two OFDM symbols with frequency hopping configuration is used, the complex correlation values for OFDM symbols have different random initial phases. In the case when these phases are opposite, the summed value of them in (2) may significantly decrease and consequently reduce the decoder performance.

To solve the described problem, we propose to combine correlation values by their absolute values as follows:

$$P_{m_{CS}} = \frac{1}{N_{rx}N_{Sym}N_{CS}^{RB}} \sum_{r}^{N_{rx}} \sum_{i}^{N_{Sym}} \left| \sum_{k}^{N_{CS}^{RB}} R_r^i[k]\left(S_{m_{CS}}^i[k]\right)^* \right|^2 \quad (3)$$

After calculating $P_{m_{CS}}$ for all $N_{m_{CS}}$ possible values of m_{CS}, the maximum $P_{m_{CS\max}}$ is detected and compared with a threshold $ThrH$. If $P_{m_{CS\max}} \ge ThrH$, then the corresponding decoded HARQ and SR bits are obtained.

For the second task, in this study we use a deciding threshold, whose value varies depending on the received signal and noise power. This approach is quite applicable for practical scenarios, such as the dependency of received signal power on UE location together with unexpected variation of

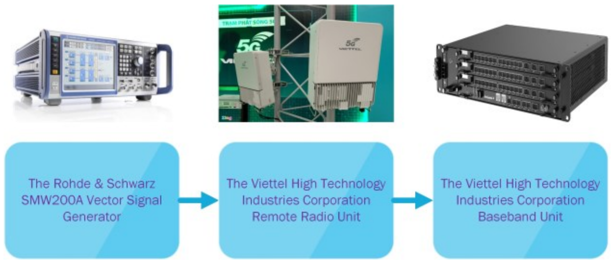

Fig. 2 Practical scheme for performance evaluation.

background noise power from radio unit. Specifically, the deciding threshold is calculated as follows:

$$ThrH = \frac{K}{N_{m_{CS}}} \sum_{m_{CS} \neq m_{CS_{\max}}}^{N_{m_{CS}}} P_{m_{CS}} \tag{4}$$

where: K is a scaling factor, which is statistically chosen to satisfy the criteria of DTX detection probability.

To evaluate the decoding performance of two algorithms (2) and (3) using the deciding threshold in (4), we use $P_{Miss.Dect}$ (the probability of not correctly decoding ACK bits when ACK bits were sent) and P_{DTX} (the probability of erroneous decoding ACK bits when only noise at the input) as defined by 3GPP in [11]. It is required that $P_{Miss.Dect}$ and P_{DTX} are less than 1% at a given SNR depending on system configuration.

III. Practical Experiment Description

In order to verify performance of the proposed method, this paper carries out experimental results with the aid of the SMW200A Vector Signal Generator from Rohde & Schwarz.

As shown in Fig. 2, experimental prototype includes three main blocks: the SMW200A Vector Signal Generator, the remote radio unit (RRU) and the baseband unit (BBU) from Viettel High Technology Industries Corporation (VHT). While the SMW200A generates the desired signal with specific environment, the VHT RRU captures time-domain signal and converts it into base-band frequency-domain signal by means of the FFT stage. After obtaining frequency resource grid, the VHT BBU plays vital role in decoding signal since it is utilized to implement the control source code.

TABLE II and TABLE III respectively provide detail system parameters as well as the evaluated test cases in this work. As mentioned earlier, this study only discusses the PUCCH format 0 using two OFDM symbols with different intra-slot frequency hopping configurations. On the other hand, effectiveness of the proposed approach is also clarified in terms of various number of reception antenna.

TABLE III
System Parameters for Performance Evaluation

System parameters	
Carrier Frequency	3.7 GHz
Channel Bandwidth	100 MHz
Subcarrier Spacing	30 kHz
FFT size	4096
Number of Tx Antennas	1
Number of Rx Antennas	1/2/4
Signal Power	-70 dBm

TABLE II
Test Case Parameters for Performance Evaluation

Parameters	Testcase 1	Testcase 2	Testcase 3
Number of HARQ/SR Bits	1	1	1
Number of Resource Block	1	1	1
Frequency Hopping	Enable	Disable	Enable
Number of Rx Antennas	2	2	1/2/4
Number of OFDM Symbols	2	2	2
Channel conditions	TDLC300 – 100 Low	TDLC300 – 100 Low	TDLC300 – 100 Low

IV. Results And Discussion

This paper conducts three test cases whose detail parameters are listed in table II from left to right, respectively. Frequency hopping is the difference between two first test cases, and test case 3 is about decoding performance with various Rx antenna numbers. In the following sessions, method 1 and 2 stand for the conventional and the proposed methods whose cyclic shift correlation values are given in (2) and (3), respectively. After calculating correlation of each cyclic shift, DTX status is decided with the aid of the threshold derived in (4).

A. Test case 1

In this test case, PUCCH format 0 with the enabled intra-slot frequency hopping is under consideration.

As depicted in Fig. 3, the conventional method 1 approximately keeps $P_{Miss.Dect}$ at 5.5% with the $3.5dB$ SNR in case of $2Rx$ antennas. In other words, it does not comply with the TS 38.104 chapter 8 requirement in which $P_{Miss.Dect}$ has to be lower than 1%. In contrast, the proposed method 2 offers significant improvement with very low $P_{Miss.Dect}$ as plotted in Fig. 3, $P_{Miss.Dect}$ is pinned at 0.3% by means of the absolute summation in (3). As a result, it can be concluded that the proposed strategy strongly ensures the requirement described in the TS 38.104 chapter 8.

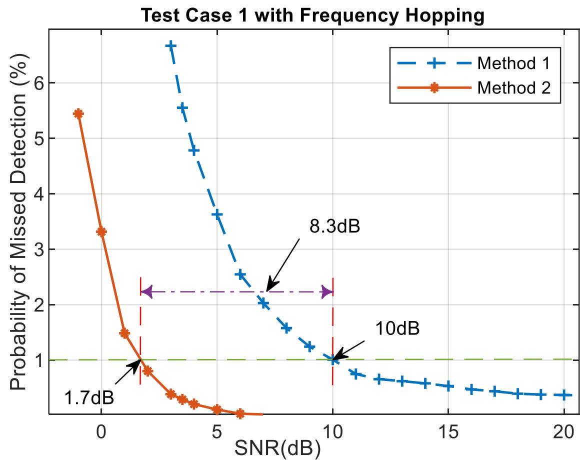

Fig. 3 Results for 2Rx with frequency hopping.

Along with the results at the $3.5dB$ SNR, Fig. 3 also provides $P_{Miss.Dect}$ values within wide range of SNR. In Fig. 3, the proposed method 2 is not only effective but also stable since $P_{Miss.Dect}$ values stiffly moves toward to zero as SNR increase. In the same scenario, but with the applied conventional method 1, $P_{Miss.Dect}$ values are not well maintained around zero, which means poor performance. With the $8.3dB$ margin, Fig. 3 also differentiates robustness between two methods.

From Fig. 3, it can be seen that the proposed approach demonstrates absolutely high decode efficiency so that it is very suitable for 5G NR practical applications.

B. *Test case 2*

While intra-slot frequency hopping is enabled in section A, it is not allowed in this section. In this scheme, performance of both strategies are reflected in Fig. 4.

In Fig. 4, even though the conventional method 1 results in the 5% $P_{Miss.Dect}$ at $0.8dB$ SNR, it requires very high SNR value, i.e. $7.7dB$, to reach the 1% $P_{Miss.Dect}$. Therefore, the conventional method is not sufficiently robust to handle such configuration. In case of the proposed approach, decoding result is still impressive because $P_{Miss.Dect}$ reaches the 1% value at the $4.8dB$ SNR. In terms of margin, as described in Fig. 4, the proposed method 2 gains $2.9dB$ margin which is safe and sufficient for operating under different conditions.

In addition, Fig. 3 and Fig. 4 differentiate performance of the proposed algorithm when intra-slot frequency hopping is respectively configured/not configured. From these figures, intra-slot frequency hopping leads to higher decoding effectiveness, so that it is highly recommended for countering fading interference.

From the above explanation, it can be realized that the proposed method 2 remains better performance in comparison with the conventional method 1 in both intra-slot frequency-hopping configurations. In other words, it is not only versatile but also highly advanced.

C. *Test case 3*

Besides different frequency hopping configurations, this work also considers decoding performance under variable Rx

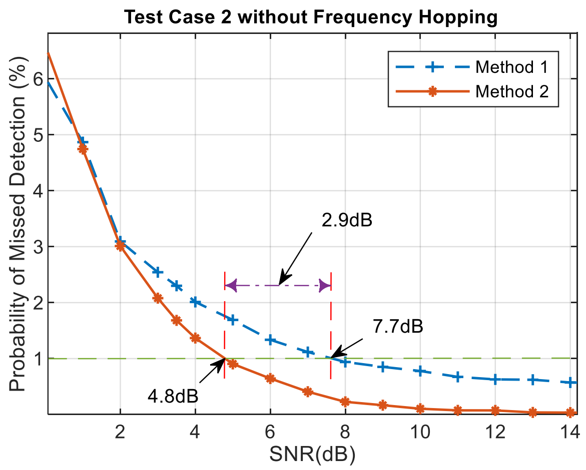

Fig. 4 Results for 2Rx without frequency hopping.

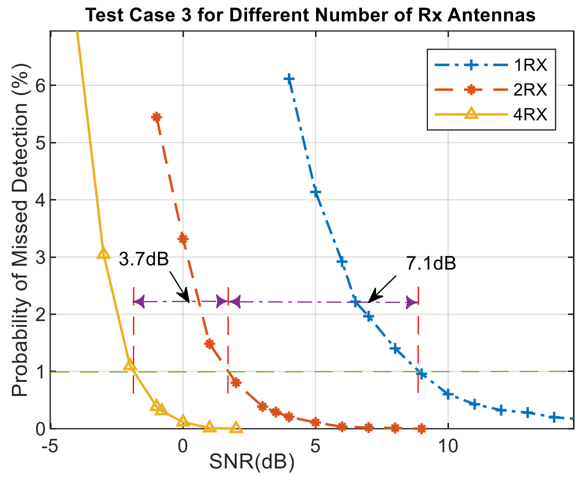

Fig. 5 Results for 1-2-4 Rx with frequency hopping.

antenna number condition. In this regard, Rx antenna number changes from 1 to 2 and 4 while intra-slot frequency hopping is enabled to adopt the TS 38.104 parameters requirement. Detail experimental results are given in Fig. 5.

In Fig. 5, decoding performance steadily increases by number of Rx antenna. As we know, the TS 38.104 also describes requirement for the $4Rx$ case in which $P_{\text{Miss.Dect}}$ is lower than 1% at the $-0.8dB$ SNR. Thanks to the proposed method, $P_{Miss.Dect}$ is kept at 0.3% with the specified SNR as introduced in Fig. 5 in case of $4Rx$. Meanwhile, $P_{Miss.Dect}$ .is kept at 0.3% with the $12.5dB$ SNR when only $1Rx$ is employed. Performance difference among three Rx antenna numbers is also brought out by considering their PACK at 1% as plotted in Fig. 5.

From the above analysis, it can be seen that the proposed approach fully covers the TS 38.104 standard in terms of PUCCH performance requirements for format 0 with multiple Rx antennas.

V. Conclusions

This paper proposes a practical method that significantly enhances decoding performance by summing absolute values of symbols power. By considering different operating conditions, experimental results are brought out to demonstrate the advantages of the proposed approach. In case of frequency hopping configuration, ACK missed detection probability well complies with the TS 38.104 standard since it is much lower than 1%. Moreover, effectiveness of the proposed method 2 is also verified when Rx antenna number varies with different values. The proposed method 2 offers dramatic improvement with the least modification in control source code, which means very high convenience and versatility. Therefore, the proposed method 2 is highly practical and applicable in industry.

VI. Acknowledgment

The authors would like to thank to Viettel 5G CPU Signal Processing Physical Layer colleagues for valuable discussions and comments. This work was supported by 5G NR gNodeB project of Viettel High Technology Industries Corporation, Viettel Group. The technologies described in this paper are owned by Viettel High Technology Industries Corporation, Viettel Group.

REFERENCES

[1] 3GPP, TS 38.300 v16.5.0, "NR and NG-RAN Overall Description (Release 16)" March 2021.

[2] L. Wang, Y. Matsumura, K. Takeda, X. Hou and S. Nagata, "Uplink control channel for 5G new RAT," 2017 11th International Conference on Signal Processing and Communication Systems (ICSPCS), Surfers Paradise, Australia, 2017, pp. 1-7.

[3] D. Gurgunoglu and S. Gezici, "Channel Estimation Methods for 5G Physical Uplink Control Channels," 2020 28th Signal Processing and Communications Applications Conference (SIU), Gaziantep, Turkey, 2020, pp. 1-4.

[4] A. Krylov, A. Rashich, A. Gelgor and D. Fadeev, "Polar Codes Sequential Decoder Hardware Architecture," 2019 42nd International Conference on Telecommunications and Signal Processing (TSP), Budapest, Hungary, 2019, pp. 261-264.

[5] L. Kundu, G. Xiong and J. Cho, "Physical Uplink Control Channel Design for 5G New Radio," 2018 IEEE 5G World Forum (5GWF), Silicon Valley, CA, USA, 2018, pp. 233-238.

[6] Y. Matsumura, L. Wang, K. Takeda and S. Nagata, "5G new RAT uplink control channel for small payloads," 2017 11th International Conference on Signal Processing and Communication Systems (ICSPCS), Surfers Paradise, Australia, 2017, pp. 1-5.

[7] Y. -H. Kim, H. Ju, C. B. Jeong and M. -S. Lee, "Performance comparison of DTX detection schemes for 5G NR PUCCH," 2020 International Conference on Information and Communication Technology Convergence (ICTC), Jeju, Korea (South), 2020, pp. 1391-1394.

[8] 3GPP TS 38.211 v16.3.0, "Physical channels and modulation," 09-2020.

[9] T. A. Pham and B. T. Le, "A proposed preamble detection algorithm for 5G-PRACH," 2019 International Conference on Advanced Technologies for Communications (ATC), Hanoi, Vietnam, 2019, pp. 210-214.

[10] M. Hua et al., "Analysis of the Frequency Offset Effect on Random Access Signals," in IEEE Transactions on Communications, vol. 61, no. 11, pp. 4728-4740, November 2013.

[11] 3GPP, TS 38.141-1 V16.5.0 (2020-09) "Base Station conformance testing".

[12] 3GPP, TS 38.104-1 V17.0.0 (2020-12) "Base Station radio trasmission and reception".